SPACE DEBRIS ATTITUDE DETERMINATION OF FAINT LEO OBJECTS USING PHOTOMETRY: SWISSCUBE CUBESAT STUDY CASE

Jean-Noël Pittet[(1)], Jiří Šilha[(1)], Thomas Schildknecht[(1)], Muriel Richard[(2)], Dimitri Hollosi Antal[(2)], Christophe Paccolat[(3)], Volker Gass[(3)], and Jean-Philippe Thiran[(4)]

[(1)]*Astronomical Institute, University of Bern, CH-3012 Bern, Switzerland, Email: {jean-noel.pittet, jiri.silha, thomas.schildknecht}@aiub.unibe.ch*
[(2)]*eSpace, EPFL, 1015 Lausanne, Switzerland, Email: muriel.richard@epfl.ch*
[(3)]*Swiss Space Center, EPFL, 1015 Lausanne, Switzerland, Email: christophe.paccolat@epfl.ch*
[(4)]*Signal Processing Lab (LTS5), EPFL, 1015 Lausanne, Switzerland*

ABSTRACT

Knowledge about the attitude state of space debris is necessary for the design of active debris removal missions. Ground-based, passive optical observations may be used to improve the accuracy of orbital predictions and allow studying the attitude motion of spinning passive objects in orbit. The application of developed methods can be extended to contingency scenarios (failure investigation) or even to active mission, for example for the validation of sensors. Unlike other methods that use retro reflectors on the target or complex radar facilities, the method used in this work requires only a telescope equipped for relative[1] photometry. Acquisition routine should include tracking algorithms for the targeted orbits.

Other teams using similar methods studied primarily the large objects, which spin fast or which move slowly in the sky. Challenges related to acquisition and processing increase when small objects in low Earth orbit are studied as the phase angle varies quickly with time, the signal can be very faint and the spin axis is typically less stable due to external perturbations. In addition, the complexity of the analysis increases when the targets are spinning slowly. Between April and July 2016, SwissCube, a 10cm CubeSat type spacecraft designed, built and operated by EPFL (École polytechnique fédérale de Lausanne) and other Swiss partner institutions, has been intensively observed by the Astronomical Institute of the University of Bern (AIUB). EPFL was retrieving internal attitude data and performing radio signal amplitude analysis for the time intervals of the AIUB optical observations. These three independent sources of attitude estimation were combined for validation purposes. The spin rate has been actively changed during this period in order to test the limits of this method for different spin periods.

This paper presents the observation (photometry and radio signal) and the data processing techniques in the first section. It then describes the SwissCube sensors and their configuration in the Cube. Finally, we present the observations and cross-correlation results. The results are encouraging, especially for SwissCube spin rates greater than 6 deg/sec.

Keywords: attitude determination; attitude control; photometry; SwissCube; CubeSat.

1. INTRODUCTION

To measure the attitude state for space objects, currently several types of measurements are used. Some of them can provide the direct information for the spin behaviour, like SLR measurements to cooperative targets [11] or Inverse Synthetic Aperture Radar (ISAR) images performed by radar [7, 10]. Direct optical imaging after processing may provide similar results as the ISAR images. Most cost effective for long time monitoring of the objects behaviour and its evolution are the optical telescope measurements. For optically varying targets, such as rotating spacecraft, upper stages or orbital fragmentation part, a sequence of photometric measurements needs to be acquired within a time interval of few minutes with small time step (few seconds), depending on the orbit and attitude of the target. Such measurement is called a light-curve, i.e. the brightness variation during the measurement time. Light curves are strongly related to the spin attitude of the observed object. This is why this is a promising technique to determine rotation or tumbling rates. To be able to analyse light curves obtained by optical measurements, i.e. determining the rotation period and the rotation axis direction, several methods can be applied [8]. Example of a light curve acquired by AIUBs ZIMLAT system (see section 2.1) is plotted in Fig. 1.

Photometry on CubeSat has been previously studied for discrimination of multiple deployment [3]. In this paper, the light-curves are used to recognized different simulated cubeSat with different antennae pattern (0, 6 or

[1] i.e. the absolute magnitude calibration is not needed.

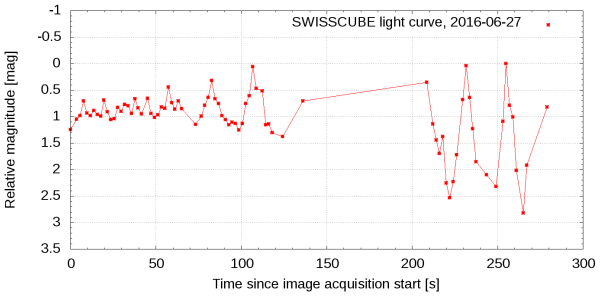

Figure 1. SwissCube light curve acquired by ZIMLAT telescope during the night of the 2016-06-27.

8). Recently, CubeSat light curves have been successfully obtained from a low cost electro-optics system [1]. The authors developed a photometric system based on a mobile amateur telescope and create an open source processing chain.

1.1. SwissCube

SwissCube is the first satellite which was completely developed and built in collaboration with several educational institutions in Switzerland. Led by the Ecole Polytechnique Federale de Lausanne, the HES-SO, the University of Neuchatel and the FHNW took part in the development of this CubeSat. The satellite was successfully launched by the Indian Polar Satellite Launch Vehicle (PSLV-C14) on 23rd of September 2009 as a secondary payload together with three other CubeSats. SwissCube was inserted into a 720 km polar sun synchronous orbit. SwissCubes payload is a small telescope that took intensity images of the airglow phenomena caused by the recombination of atomic oxygen in the Earths upper atmosphere. Fig. 5 shows the layout and elements of SwissCube. SwissCube was launched in a close to 12-noon plane in 2009 and as shown in Fig. 2, the orbital perturbations decayed the semi-major axis and moved the orbital plane to approximately a 2:40-14:40 orbit in 2017. This orbit made ground optical observations possible only during particular periods.

1.2. Rotation physics

Let's recall that in the tensor of inertia (MOI) of a solid body, the eigenvector are supporting the so-called inertia axis I_1, I_2, I_3. Their eigenvalues are their corresponding momentum of inertia. The principal axis of inertia (I_1) is the one with the greater eigenvalue. The Euler theorem teach that an instantaneous rotation axis $\hat{\omega}$ can always be defined. When the rotation axis is not aligned with an inertial axis, the rotation axis will have a jitter motion called (free) nutation. On the opposite, for a rotation without nutation, $\hat{\omega}$ is aligned with an inertia axis. For a body with $I_1 > I_2 > I_3$, only the rotations around I_1 and I_3

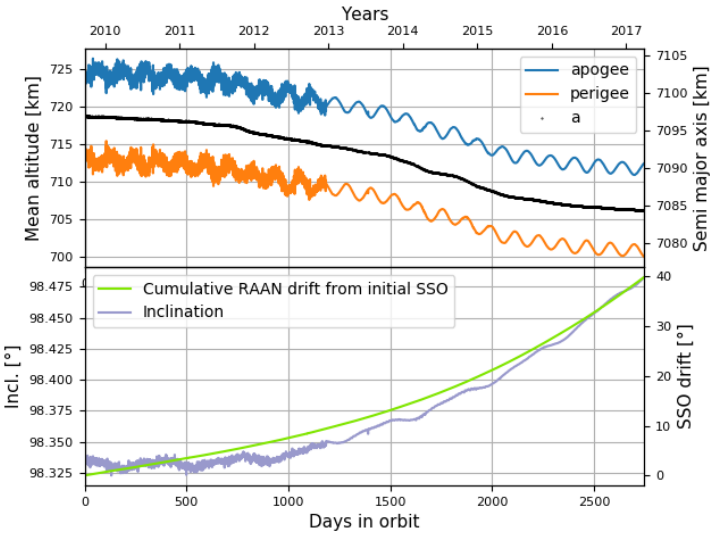

Figure 2. SwissCubes orbital elements drifts between launch in 2009 and early 2017. Based on TLE data form [13]

are stable, *i.e.* $\hat{\omega}$ is constant. This situation is called a flat spin.

In practice, dissipative forces, like friction in cables or sloshing, can damp the nutation. The rotation around I_1 is observed to be more probable than I_3. With those considerations, one can often use the working assumption of a flat spin around the principal axis of inertia.

1.3. Ground based attitude determination

Traditional attitude determination is usually defined to be equivalent to find the rotation matrix from the engineering body frame to the "real world" inertial reference frame. This study actually try to determine the attitude kinematics. It need six quantities to be fully represented. The chosen parametrisation is:

- $|\vec{\omega}|$, the spin rate. Alternatively, the related period can be given.
- $\hat{\omega_I}$, the normalized spin vector in the inertial reference frame. The TEME was chosen for the simplicity of the usage with TLE data.
- $\hat{\omega_B}$, the normalized spin vector in the body reference frame.
- ϕ, a phase angle at a given epoch.

With $|\vec{\omega}| = |\vec{\omega_I}| = |\vec{\omega_B}|$. Those parameters are particularly suited for flat spin, on which case they are constant without perturbation torques. They also reflect the determination process where, usually the spin rate is found first, and then the other parameters. Often, ϕ is ignored

as it do not bring any information about the body rotation dynamics.

Due to its orbital motion, a LEO satellite will appear rotating around an observer on the ground. This will introduce an apparent rotation of the target. The period observed from ground is then refereed as the apparent period. This notion is similar to the sidereal and synodic orbital periods. A accurate estimation of this effect require the knowledge of the spin axis. However, the order of magnitude can be estimated as an additional half rotation over one pass by the following equation:

$$\frac{P_{app}}{P_{inert}} = \frac{N_{inert}}{N_{app}} \approx \frac{N_{inert}}{N_{inert} \pm 0.5} \tag{1}$$

Where P stand for the periods and N the number of rotations observed during one pass. The subscript $_{app}$ and $_{inert}$ are for apparent respectively inertial spin rotation. For a pass of 10 minutes and a spin period of 30 seconds, this represent average apparent period of 31.5 seconds (2.5%). This is a mean value, as the instantaneous ratio depend of the geometry of the pass (target trajectory, observer position, spin axis orientation) and is relative to the angular motion. Which means that far from the zenith portion of the pass, where the angular motion is slow, this effect is weaker. It's then difficult to define rigorously the apparent period on the base of the inertial one, and for doing so, one should already know the spin axis in the inertial reference frame ($\hat{\omega_I}$). Hopefully, in practice the difference is small enough, and comparison of both values can serve for validation, without more refined model.

2. METHODS DESCRIPTION

2.1. ZIMLAT telescope processing chain

AIUBs Zimmerwald Observatory consists of two main optical systems, the 1-m Zimmerwald Laser and Astrometry Telescope (ZIMLAT) 3 and the 0.2-m Zimmerwald Small Aperture Robotic Telescope (ZimSMART).

ZIMLAT is used either for satellite laser ranging (SLR) [7] or for optical observation (astrometric positions and magnitudes) of artificial and natural objects in near-Earth space. During daytime, the system operates in SLR mode only. During night time, the available observation time is shared between the two modes based on target priorities. In addition, light curves and photometric observations can be acquired on demand. For ZIMLAT there are two different tracking modes: the sidereal and object tracking. The latest require the coordinates and velocities ephemeris generated in advance. For the acquisition of SwissCube light curves, a Charged Coupled Device (CCD - SI1100) camera was used. The automatic AIUB/ZIMLAT processing chain extracted the intensities from the frames and constructed the light curves.

Figure 3. AIUBs 1-meter ZIMLAT telescope dedicated to the photometric and astrometric measurements.

By using proper processing one can extract the rotational frequencies from light curves for the majority of the targets, which are visible for the telescope. AIUB is using several methods to extract apparent period from light curves. A first set of methods used to detect periods from light curves, are the Fast Fourier Transformation (hereafter FFT), the Periodogram analysis and Welch's method. These three approaches were chosen as a starting point to get familiar with time series analyses, as they are widely used in scientific community. All three mentioned methods are based on the Fourier transform and need therefore equally spaced data in time as an input. The light curves being unevenly spaced, some preprocessing is needed before further processing.

There are several types of approaches which are able to deal with unevenly spaced data. Among them, one find the so-called Folding methods, with in particular the Epoch folding and the Lafler-Kinman method. After further investigation it was decided to implement the Epoch folding, because the results shown by S. Larsson [5] preferred this method over Lafler-Kinman method. For more about the space debris light curves acquisition and processing please refer to [8, 12].

The apparent rotation periods in this study have been obtained by using method of epoch folding [5]. Results of epoch folding of the light curve plotted from Fig. 1 can be seen in Fig. 4. In this example, the processing revealed apparent rotation of SwissCube to be 11.9 s which corresponds to 30.3 deg/s rotation angular velocity.

2.2. SwissCube internal measurements

SwissCubes attitude determination and control (ADCS) was fitted with three orthogonally placed custom designed magneto-torquers and a 3-axis Honeywell HMC1043 magnetometer. The attitude control is based on a simple B-dot controller. To complement magnetic measurements, three 1-axis Analog Digital ADXRS401 MEMS gyroscopes were added to provide angular rate measurements (see Fig. 6) and a set of sun-sensor, one on each six faces, were install. The outputs of the two latter however were not used in the satellite attitude control

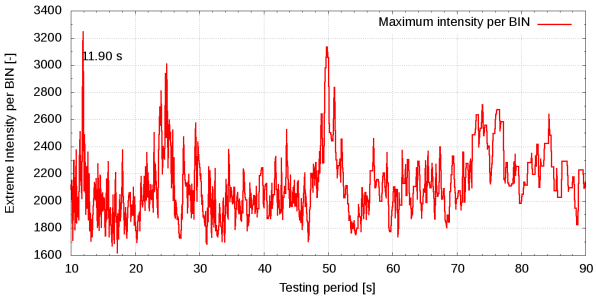

Figure 4. Epoch folding procedure output for SwissCube light curve acquired by ZIMLAT telescope at 2016-06-27. The peak at 11.9 second is the fundamental period. Two harmonic peaks are visible.

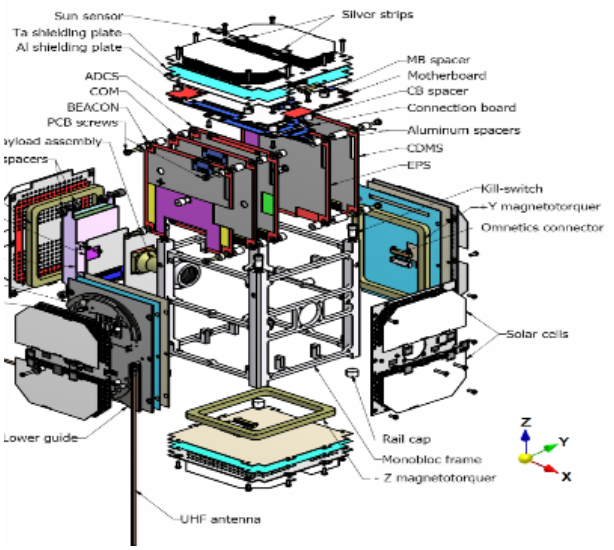

Figure 5. SwissCube subsystems and layout

system. The B-dot control algorithm design was tuned to allow for a small residual rotation (down to 1 deg/s). This would ensure that the camera payload would eventually point at different parts of the atmosphere. However, the B-dot controller is by default not engaged, meaning that it is typically turned on and off by a ground command. Most of the time it is turned off to conserve power, thus perturbations have been observed to accelerate SwissCube rotations to quite a high level. When that happens, the B-dot is then actuated by a command from the ground and the satellites rotation slows down [6]

All sensor measurements are temperature-compensated on the ground. During the development phases, each sensor was individually characterized. A great care was taken during the testing of the magnetometer, since it is the main sensor for the B-dot controller. Throughout the qualification and acceptance testing of the ADCS, a temperature dependant drift was observed in the gyroscopes data. These behaviours found during the characterization have been used in the post-processing analyses to filter the gyros data, knowing the operation temperature (a quantity that is also measured). Based on the ground and

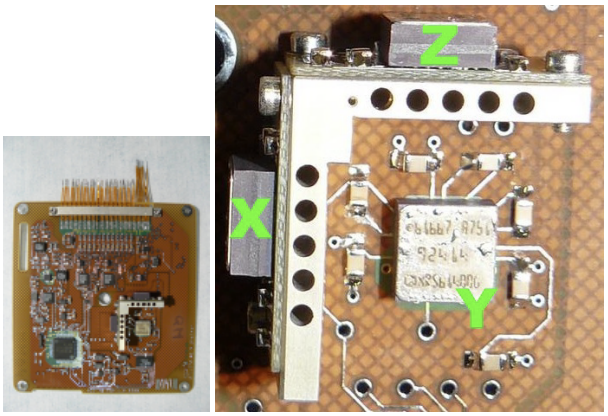

Figure 6. SwissCube ADCS board (left) with the gyroscopes mounted along the three directions (right).

flight results, the uncertainty on the gyroscopes measurement and reconstruction is estimated at about $\pm$ 1deg/s.

As some other housekeeping data, the gyros data was not stored in the memory and thus it is only available when requested by the ground when the satellite is passing over the station. The operations in 2016, the period of interest to this paper, were done by a Radio-Amateur in Switzerland (HB9MFL).

2.3. Radio signal

To complement the gyroscope data, which in some cases was not available at the time of the optical ground observations, an analysis of the received RF signal was performed. It was indeed possible to deduce SwissCubes rotation based on the downlink signal as described below. The SwissCube satellite has two main communication links. The first link is a low power beacon signal in Morse code, generated by the EPS board and transmitted by the Beacon board. The beacon is composed of 4 different messages containing basic housekeeping data. These messages are constantly transmitted one at a time every 30 seconds. The second is the high-power and high data rate RF link (uplink and downlink), generated by the COMmunication board. This link is initiated by a ground command, and thus is only available when over a commanding ground station (at the time of observation, in Switzerland by Radio Amateur HB9MFL). For both beacon and main high data rate modes, the uplink signal uses the VHF 145 MHz carrier frequency and is modulated using AFSK. The downlink signal sends the scientific and engineering telemetry at 1200 bits/sec at an RF output power of 30 dBm (1W) and modulates the UHF signal in FSK at a frequency of about 437 MHz. Thus two different antennae are used for uplink and downlink. Of interest here is the downlink UHF antenna pattern. The UHF antenna is a quarter-length monopole 176 mm long. Its gain is 3.15 dBi. As shown in the layout of the satellite (Fig. 5), the UHF antenna was mounted on the Y face and is aligned with the Z-axis. The measured pattern based on

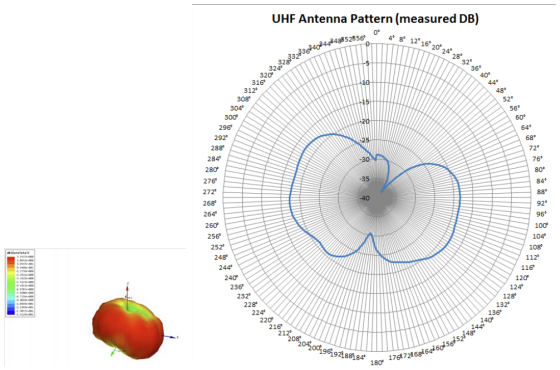

Figure 7. SwissCube UHF measured antenna pattern in a polar plane. The antenna was installed on the SwissCube structure and panels during tests.

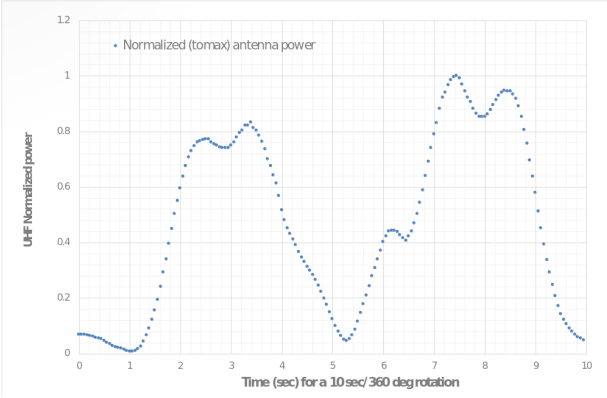

Figure 8. SwissCube UHF measured antenna pattern in a polar plane. The antenna was installed on the SwissCube structure and panels during tests.

tests done on the ground is provided in Fig. 7. These tests were performed with the two uplink and downlink antennas attached to a backplane on SwissCubes structure, thus taking into account the surrounding RF perturbations.

The UHF pattern is basically a doughnut along the axis of the monopole antenna. Maximum power will be provided along its equator, while substantial power losses are experienced while communicating in the regions of the poles of the antenna (along spacecraft Z axis). This effect is what is used to reconstruct the SwissCubes rotations from the ground. If a ground station is acquiring the downlink data as the antenna rotates in a polar plane, the relative signal strength based on the ground measurement will be as shown in Fig. 8. These effects will be particularly clear for rotation around the X or Y axis of the satellite.

Thus during passes over the ground station, the signal was analysed and a rotation period could be deduced. Note that in the perfect case of flat spins around the X or Y-axis, and viewed from the Z-axis, one rotation period is determined by the duration between three power minimum. In most cases however, the reconstruction of the SwissCube rotations will be dependent on the ground

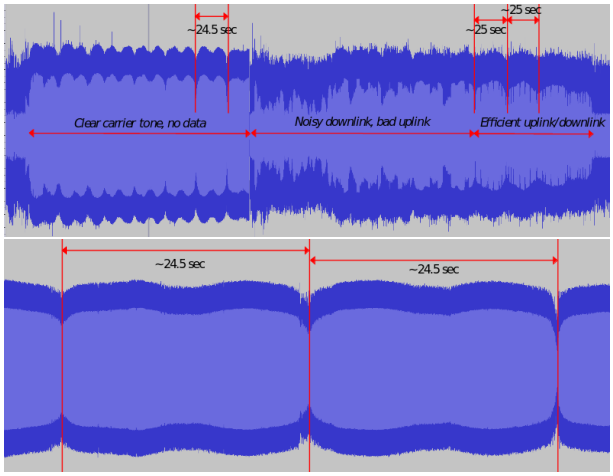

Figure 9. Visualisation of the RF power of the audio signal during pass 26-06-2016 14:52. The bottom part is a zoomed portion of the upper one.

station-to-satellite line of sight and on the pointing direction of the rotation axis of the satellite. Since the latter is unknown, there are 3 possible ways to view the rotations:

- The audio signal shows no dip, and it is not possible to define the rotation rate. This case need the rotation axis to be parallel to the antenna and to be perpendicular to the line of sight;
- The audio signal shows regular and frequent dips as shown in Fig. 9, where the separation between two (deep) dips corresponds to a full rotation;
- The audio signal shows regular and frequent dips, where the separation between two dips corresponds to a half of a rotation. This case need the observer to view the tow ends of the antenna during the rotation, *i.e.* the rotation axis to be perpendicular to the antenna and the line of sight.

The rotation rates are thus subject to an ambiguity of a factor of two. The accuracy at which the rotation can be reconstructed is estimated to within 1 sec.

3. RESULTS

In order to perform a successful optical observations, a ground station has to be in the (astronomic) night, while the satellite must be in the sunlight during sufficient time to be tracked. When a satellite is in a sun synchronous orbit (SSO), he will pass over any point of the planet around the same local solar times[2]. This imply that the passes visible from a single observatory on Earth, always occur around given hours of the day.

[2]This is particularly true for points on the Earth equator, where the passes are 12 hours apart.

Table 1. Periods extracted from light-curves. The numbers in parenthesis are the other peaks present rejected by the analysis.

Date (UTC)	App. period	
30/04/2016 · 00:49	-	not enough data
05 05 2016 · 01:14	∞	too slow
18 05 2016 · 01:00	-	not enough data
10 06 2016 · 01:35	58 s	$(57.2/116)$ s
28 06 2016 · 01:45	25 s	from specular
28 06 2016 · 01:45	24.9 s	$(49.8/74)$ s
04 07 2016 · 01:16	19.7 s	(37.1) s
07 07 2016 · 00:13	21.95 s	(70.1) s

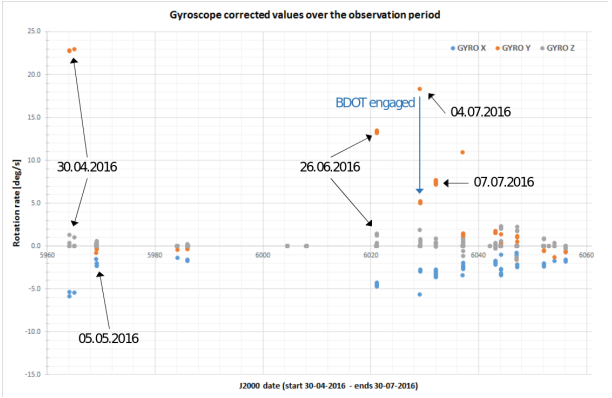

Figure 10. SwissCube's gyroscopes measurements over the observation period.

The orbit of SwissCube being almost in a perfect SSO, this is true with a small drift along the years (see Fig. 2). It was found that the appropriates conditions will be fulfil during a limited time window, from end of April 2016 to begin of July 2016. It was decided to observe every photometric opportunities, and to intensify the communications with the satellite in order to maximize the correlations opportunities. Tab. 1 show the extracted apparent periods with the folding period method as described in section 2.1. From the seven observations that could be processed, one have distinctive specular reflection peaks from the Sun (on 28 06 2016). This allow an approach slightly different.

The communications with the satellite are possible day and night. However, operations are avoid during the night to avoid a faster decay of the batteries lifetime. During the campaign, 15 attempts were successful to download at least one ADCS data set. At three occasions, the B-dot has to be turned on to damp the spin to prevent that he tumble out of control. Fig. 10 shows the measured rotation rates on the X, Y and Z axis during the period of observations.

The spin rate ($|\vec{\omega}|$) extracted from those data along with the estimation of the spin axis $\hat{\omega_B}$ are recorded on Tab. 10. The occasion when the spin of the satellite was actively reduce by the B-dot algorithm are also represented as well as on all other results tables.

Table 2. Summary of the gyroscopes internal measurements and spin stabilisation commands. The axis column show the dominant axis of rotation when it can be identified. The Y axis of the spacecraft correspond at 9° to the principal inertia axis measured on ground.

Date (UTC)	Spin rate	Period	Axis $\hat{\omega_B}$
30 04 2016 · 14:24	$23.4\ °s^{-1}$	15.4 s	Y
01 05 2016 · 13:33	$23.6\ °/s$	15.3 s	
	B-dot enable		
05 05 2016 · 13:15	$1.76\ °/s$	205 s	
05 05 2016 · 14:49	$2.22\ °/s$	162 s	
20 05 2016 · 14:28	$1.40\ °/s$	257 s	
22 05 2016 · 12:37	$1.68\ °/s$	214 s	
26 06 2016 · 13:52	$14.1\ °/s$	25.5 s	Y
04 07 2016 · 13:13	$19.3\ °/s$	18.7 s	Y
	B-dot enable		
04 07 2016 · 14:51	$5.87\ °/s$	61.3 s	Y
07 07 2016 · 13:47	$8.15\ °/s$	44.2 s	Y
12 07 2016 · 12:33	$11.5\ °/s$	31.3 s	Y
	B-dot enable		
12 07 2016 · 14:13	$2.63\ °/s$	137 s	
12 07 2016 · 15:45	$2.70\ °/s$	133 s	
18 07 2016 · 13:44	$2.39\ °/s$	151 s	
18 07 2016 · 15:20	$2.60\ °/s$	138 s	

Fig. 10 shows the measured rotation rates on the X, Y and Z axis during the period of observations.

Tab. 3 shows the results of the radio signals analysis. The gyroscopes data is used to resolve the ambiguity and for most cases, there is a good agreement between the two types of measurement.

Table 3. Measures based on radio signal.

Date (UTC)	Apparent period
30 04 2016 · 14:24	15.5 s
05 05 2016 · 14:49	Difficult to assess
20 05 2016 · 14:28	Difficult to assess
09 06 2016 · 23:57	∞
15 06 2016 · 13:57	∞
26 06 2016 · 13:52	25 s
04 07 2016 · 13:13	18.5 s
04 07 2016 · 14:51	60 s
07 07 2016 · 13:47	42 s
18 07 2016 · 15:20	85 s

4. DISCUSSION

Gyroscopes show strong indication of flat spin along Y when $|\omega|$ is over ≈ 5 deg/s. This axis correspond roughly to the principal axis measured on ground. For slower spin rate, the direction of the spin, the possible nutation motion and the measurements error were not distinguishable. So, no rigorous analyses could be made.

An other possibility of flat spin validation came from the sun sensor analysis. Six sun-sensors are installed on the face of SwissCube in order to estimate the Sun direction within the spacecraft reference frame. It was discovered recently that three of them were malfunctioning. Their data had to be ignored and so create interruption in the data.

In case of flat spin, multiple sun vectors shall fit a cone with the axis along an axis of inertia. In consequences, only the 04/07/2016 14:51 and 07/07/2016 passes have more than 3 reconstructed sun vectors from the sun sensor. The period is extracted using a period folding algorithm as described in 2.1. For the pass of the 26/06/2016, the spin rate from the sun sensor was estimated taking the assumption of a flat spin around the Y axis. Those results are displayed in the Tab. 4.

4.1. Spin rates comparison

As introduced in the section 1.2, each of those periods have a different exact definition, thought, a direct numerical comparison is not possible. In the details, the period extracted from the sun sensor is the closest to the inertial definition. The only deviation are coming from the flat spin assumption and the motion of satellite around the Earth and the Sun, what is negligible in our case. The difference with the apparent radio and photometric period come from the angular motion of the spacecraft viewed from ground. The photometric apparent period is further dependent of the phase angle (the observer - target - Sun angle).

All processed periods are displayed in Tab. 4 for comparison. Results are globally consistent. The period extracted from the light curve of the 7th July 2016 (21.95 s) is probably half the true period. This correction is in complete accordance with the periods extracted by other methods. The last pass, show large disagreement. It can be attributed to the limits of determination for slow rotating objects. For the other passes, the difference can be explained by the addition of the apparent spin, and by the imperfect synchronisation of the measurement. Spin axis reconstruction and simultaneous measurement are required for a refined comparison.

Table 4. Comparison of the extracted period. The symbol ∞ signify a period too long to be reliably observed.

Date (UTC)	RF	LC	HK	SunS
30/04/2016	15.5 s	-	15.4 s	-
05/05/2016	- / ∞	∞	205 s	-
20/05/2016 · 14:28	- / ∞	-	257 s	-
09-10/06/2016	∞	58 s	-	-
26-28/06/2016	25 s	24.9 s	25.5 s	24.7 s
04/07/2016 · 1-13h	18.5 s	19.7 s	18.7 s	-
04/07/2016 · 14:51	60 s	-	61.3	60.4 s
07/07/2016	42 s	21.95 s	44 s	42.99 s
18/07/2016 · 15:20	85 s	-	138 s	-

5. CONCLUSION

The Astronomical Institute of the University of Bern (AIUB) use photometry in order to determine the attitude of uncontrolled orbiting objects. Over the diversity of the potential targets, cubeSat represent a particular challenge for being small and then faint, and for their fast angular motion. SwissCube is a operational cubeSat, operated from Switzerland, equipped with internal attitude determination sensors. A suitable observation window was found from end of April 2016 to begin of July 2016 during which an intensive measurement campaign was set in order to correlate the measurements. Three independent methods were used and lead to consistent spin rate.

With the study, we succeed to both validated the attitude determination of SwissCube and to extend the photometric attitude determination capacity of AIUB to CubeSat when the spin period in under 60 s or equivalently $6^\circ s^{-1}$.

ACKNOWLEDGMENTS

The authors would like to thanks Armin Roesch (HB9MFL) who volunteer for the intense measurement campaign with his ham radio station.

REFERENCES

1. Gasdia F., Barjatya A., Bilardi S., (2016). Time-resolved CubeSat photometry with a low cost electro-optics system In *Proc. Advanced Maui Optical and Space Surveillance Technologies Conference* , held in Wailea, Maui, Hawaii, September 16-19, 2016.
2. Gurtner W., Pop E., Utzinger J., (2002) Improvements in the automation of the Zimmerwald SLR station. In *Proc. 13th International Workshop on Laser Ranging*, Maryland, NASA Conference Publication.
3. Hall D. (2008), Optical CubeSat Discrimination. In *Proc. Advanced Maui Optical and Space Surveil-*

lance Technologies Conference, held in Wailea, Maui, Hawaii, September 16-19, 2008.

4. Kanzler R., Schildknecht T., Lips T., Fritsche B., Šilha J., Krag H., (2014) Space Debris Attitude Simulation - IOTA (In-Orbit Tumbling Analysis), In *Proc. of the Advanced Maui Optical and Space Surveillance Technologies Conference*, Wailea, Maui, Hawaii, September 15-18, 2014.

5. Larsson S., (1996). Parameter Estimation in Epoch Folding Analysis, *Astronomy and Astrophysics*, Supplement series **117**, 197-201.

6. Overlack A.E., Kuiper J.M., Peter-Contesse H., Noca M., (2011). Analysis of the Attitude Control Stability of the SwissCube Nano Satellite. In *Proc. of the 1st IAA Conference on University Satellites Missions and CubeSat Workshop in Europe*, Rome, Italy, January 2011.

7. Pittet JN., Šilha J., Schildknecht T., (2017). Single pass attitude determination of ENVISAT satellite trough the laser ranging measurements, *Advances in Space Research*, in preparation.

8. Linder E., Šilha J., Schildknecht T., Hager M., (2015). Extraction of Spin Periods of Space Debris from Optical Light Curves. In *Proc. of 66th International Astronautical Congress*, Jerusalem, Israel, 2015.

9. Schildknecht T., Koshkin N., Korobeinikova E., Melikiants S., Shakun L., Strakhova S., Linder E., Šilha J., Hager M., (2015) Photometric Monitoring of Non-resolved Space Debris and Databases of Optical Light Curves. In *Proc. of the Advanced Maui Optical and Space Surveillance Technologies Conference*, held in Wailea, Maui, Hawaii, September 15-18, 2014. Ed.: S. Ryan, The Maui Economic Development Board, id.25

10. Šilha J., Pittet JN., Schildknecht t., Cerutti-Maori D., Rosebrock J., Sommer S., Leushacke L., Krag H., (2017). Comparison of the Attitude Motion of Defunct Satellites Estimated Independently from Different Types of Measurements. In *Proc. of 7th European Conference on Space Debris*, Darmstadt, Germany, 2017.

11. Šilha J., Schildknecht T., Pittet JN., Kirchner G., Steindorfer M., Kucharski D., Cerutti-Maori D., Rosebrock J., Sommer S., Leushacke L., Krrng P., Kanzler R., Krag H., (2017). Debris Attitude Motion Measurements and Modelling by Combining Different Observation Techniques. In *Proc. of 7th European Conference on Space Debris*, Darmstadt, Germany, 2017.

12. Šilha J., Schildknecht T., Pittet JN., Rachman A., Hamara M., (2017). Extensive light curve database of Astronomical Institute of the University of Bern. In *Proc. of 7th European Conference on Space Debris*, Darmstadt, Germany, 2017.

13. Space-track tool from Joint Space Operations Center. Online at *http://www.space-track.org*